JPET Fast Forward. Published on October 16, 2019 as DOI: 10.1124/jpet.119.261149
This article has not been copyedited and formatted. The final version may differ from this version.

Pharmacological profile of the novel antiepileptic drug candidate padsevonil – interactions with synaptic vesicle 2 proteins and the $GABA_A$ receptor

Martyn Wood, Veronique Daniels,* Laurent Provins, Christian Wolff, Rafal M Kaminski,† Michel Gillard

UCB Pharma, Neurosciences Therapeutic Area, Braine l'Alleud, Belgium (MW, VD, LP, CW, RMK, MG)

JPET Fast Forward. Published on October 16, 2019 as DOI: 10.1124/jpet.119.261149
This article has not been copyedited and formatted. The final version may differ from this version.

Running title (not to exceed 60 characters, including spaces and punctuation)

Padsevonil interactions with its therapeutic targets (53 characters)

Corresponding author

Michel Gillard
UCB Pharma
Chemin du Foriest
1420 Braine l'Alleud
Belgium
michel.gillard@ucb.com

Number of:

Text pages – 14 pages (main text, excluding abstract, significance statement, references, tables and figures)

Tables – 4

Figures – 6

References – 47

Number of words in:

Abstract – 249 words [250 limit]

Introduction – 591 words [750]

Discussion – 1505 words [1500]

Significance statement – 80 words [80]

List of nonstandard abbreviations

AED antiepileptic drug
BRV brivaracetam
BZD benzodiazepine
LEV levetiracetam
PSL padsevonil
SV2 synaptic vesicle protein 2

Recommended section assignment to guide the listing in the table of contents

Neuropharmacology

JPET Fast Forward. Published on October 16, 2019 as DOI: 10.1124/jpet.119.261149
This article has not been copyedited and formatted. The final version may differ from this version.

ABSTRACT

Padsevonil is an antiepileptic drug (AED) candidate synthesized in a medicinal chemistry program initiated to rationally design compounds with high affinity for synaptic vesicle 2 (SV2) proteins and low-to-moderate affinity for the benzodiazepine binding site on $GABA_A$ receptors. The pharmacological profile of padsevonil was characterized in binding and electrophysiological experiments. At recombinant SV2 proteins, padsevonil's affinity for SV2A was higher than that of levetiracetam and brivaracetam (pKi 8.5, 5.2 and 6.6, respectively). Unlike the latter AEDs, both selective SV2A ligands, padsevonil also displayed high affinity for the SV2B and SV2C isoforms (pKi 7.9 and 8.5, respectively). Padsevonil's interaction with SV2A differed from that of levetiracetam and brivaracetam; it exhibited slower binding kinetics – dissociation $t_{½}$ 30 min from the human protein at 37˚C, compared with <0.5 min for levetiracetam and brivaracetam – and its binding was not potentiated by the allosteric modulator UCB1244283. At recombinant $GABA_A$ receptors, padsevonil displayed low-to-moderate affinity (pKi 6.4) for the benzodiazepine site, and in electrophysiological studies, its relative efficacy compared with zolpidem (full agonist reference drug) was 40%, indicating partial agonist properties. In in vivo (mice) receptor occupancy studies, padsevonil exhibited SV2A occupancy at low (ED_{50} 0.2 mg/kg), and benzodiazepine site occupancy at higher doses (ED_{50} 36 mg/kg), supporting in vitro results. Padsevonil's selectivity for its intended targets was confirmed in profiling studies, where it lacked significant effects on a wide variety of ion channels, receptors, transporters and enzymes. Padsevonil is a first-in-class AED candidate with a unique target profile allowing for pre- and postsynaptic activity.

JPET Fast Forward. Published on October 16, 2019 as DOI: 10.1124/jpet.119.261149
This article has not been copyedited and formatted. The final version may differ from this version.

SIGNIFICANCE STATEMENT

Padsevonil is an antiepileptic drug candidate developed as a single molecular entity interacting with both pre- and postsynaptic targets. Results of in vitro and in vivo radioligand binding assays confirmed this target profile – padsevonil displayed nanomolar affinity for the three synaptic vesicle 2 protein isoforms (SV2A, B and C) and micromolar affinity for the benzodiazepine binding site on $GABA_A$ receptors. Furthermore, padsevonil showed higher affinity for, and slower binding kinetics at SV2A than the selective SV2A ligands, levetiracetam and brivaracetam.

KEY WORDS

allosterism, anticonvulsants, benzodiazepines, recombinant proteins, molecular drug targeting, ion channels

JPET Fast Forward. Published on October 16, 2019 as DOI: 10.1124/jpet.119.261149
This article has not been copyedited and formatted. The final version may differ from this version.

INTRODUCTION

Levetiracetam (LEV) was the first antiepileptic drug (AED) shown to exert its therapeutic activity by targeting elements of the synaptic release machinery, namely through binding to the synaptic vesicle 2A (SV2A) protein (Lynch et al., 2004). SV2A, and the other two protein isoforms – SV2B and SV2C – are integral membrane glycoproteins present in secretory vesicles of neurons and endocrine cells (Bartholome et al., 2017). The precise function of the proteins remains elusive; however, given their presence in secretory vesicles, it is most likely that they play a role in vesicle exocytosis, an observation substantiated by accumulating evidence (Mendoza-Torreblanca et al., 2013). SV2A knockout mice die in a matter of weeks; however, in vitro recordings of neurons from very young SV2A knockout mice reveal a reduction in the frequency and amplitude of spontaneous inhibitory postsynaptic currents, potentially indicating a negative effect on GABA release from presynaptic neurons (Crowder et al.,1999). Data from animals lacking both SV2A and SV2B suggest that the absence of these proteins leads to presynaptic Ca^{2+} accumulation during consecutive action potentials causing abnormal increases in neurotransmitter release (Janz et al.,1999a). The overall effect is a destabilization of synaptic circuits and aberrant neurotransmission (Crowder et al.,1999; Janz et al.,1999a). LEV reduces both inhibitory and excitatory postsynaptic currents in an activity-dependent manner, with the largest effect seen with the highest stimulation frequency (Meehan et al., 2012). Both LEV and brivaracetam (BRV), a more potent and selective SV2A ligand (Klitgaard et al., 2016), produce frequency-dependent slowing of vesicle exocytosis and recycling, and of synaptic transmission (Meehan et al., 2011; Meehan et al., 2012; Yang et al., 2015).

The substantial evidence for the role of SV2A in the pathophysiology of epilepsy (Loscher et al., 2016; Ohno et al., 2017) and the clinical utility of SV2A ligands in the treatment of patients with epilepsy, ensured that drug discovery programs focusing on SV2 ligands continued. One strand of research involved investigating the feasibility of designing a molecule with both pre- and postsynaptic activity via interaction with SV2 proteins and the $GABA_A$ receptor ($GABA_AR$), respectively. The rationale for targeting these proteins was based on observations that LEV markedly potentiated the activity of AEDs acting via GABAergic transmission, notably benzodiazepines (BZDs), in several animal models resulting in an improved efficacy/safety ratio (Kaminski et al., 2009a). More recent studies have shown that SV2A dysfunction due to a missense mutation (L174Q) results in a selective reduction in GABAergic transmission, rendering animals carrying the mutation highly susceptible to seizures and markedly facilitating kindling (Tokudome et al., 2016a, b).

JPET Fast Forward. Published on October 16, 2019 as DOI: 10.1124/jpet.119.261149
This article has not been copyedited and formatted. The final version may differ from this version.

In the subsequent rational medicinal chemistry design program, the focus was to develop a single molecule that could target SV2 proteins with high affinity, and postsynaptic $GABA_AR$s, specifically the BZD binding site, with lower affinity. Low-to-moderate affinity for this site, coupled with a partial agonist profile, could minimize the potential for the development of tolerance, a phenomenon known to occur with most BZDs (Gravielle 2016; Vinkers and Olivier, 2012). Lead optimization efforts led to the discovery of padsevonil (PSL), an imidazothiadiazole heterocycle coupled to a pyrrolidone moiety (Figure 1). PSL constitutes a novel chemical class, as indicated by its International Nonproprietary Name (INN), which was approved by the World Health Organization in 2017.

The objectives of the studies reported here are to characterize the interactions of PSL with its intended therapeutic targets and to determine its selectivity for these targets using an array of validated in vitro and in vivo techniques. The pharmacological profile of PSL in nonclinical models of seizures and epilepsy is reported in the accompanying article (Leclercq et al., 2019).

JPET Fast Forward. Published on October 16, 2019 as DOI: 10.1124/jpet.119.261149
This article has not been copyedited and formatted. The final version may differ from this version.

MATERIALS AND METHODS

Animals

Experimental procedures involving animals were conducted in compliance with guidance from the local ethics committee for animal experimentation according to Belgian law. All efforts were made to minimize animal suffering.

Naïve male specific pathogen free NMRI mice (Crl:NMRI[Han]; 24–35 g) and male Sprague–Dawley rats (200–300 g) were obtained from Charles River Laboratories (France). All animals were housed in a holding room under a 12-h light-dark cycle with lights on at 06:00 h. Temperature was maintained at 20–24°C, relative humidity at 40–70% and the rate of air replacement was at least 15 times an hour. Animals had ad libitum access to standard dry pellet food and tap water.

Radioligands, drugs and chemicals

The following compounds were synthesized at UCB (Braine-l'Alleud, Belgium): PSL ((4R)-4-(2-chloro-2,2-difluoroethyl)-1-{[2-(methoxymethyl)-6-(trifluoromethyl)imidazo[2,1-b][1,3,4]thiadiazol-5-yl]methyl}pyrrolidin-2-one), LEV (2S-(2-oxo-1-pyrrolidinyl)butanamide), UCB30889 ((2S)-2-[4-(3-azidophenyl)-2-oxopyrrolidin-1-yl]butanamide), BRV (2S-2-[(4R)-2-oxo-4-propylpyrrolidin-1-yl] butanamide), and UCB1244283 ((4-(3,5-dimethyphenyl)-N-(2-methoxyphenyl)-3-methylbutanamide). For in vitro studies, compounds were dissolved in DMSO, and for in vivo studies, PSL was dissolved in 0.1%TWEEN 80 in NaCl (0.9%), and LEV and BRV in saline.

[^{3}H]PSL (2.55 Ci mmol^{-1}) and [^{3}H]UCB30889 (47 Ci mmol^{-1}) were custom labeled by Aptuit (Greenwich, USA), and Amersham Biosciences (Amersham, UK), respectively. [^{3}H]Flunitrazepam (80–90 Ci mmol^{-1}) was purchased from GE Healthcare (Gent, Belgium). HEK cells (Flp-In™-293) and zeocin were purchased from Life Technologies (Merelbeke, Belgium), COS-7 cells from ECACC, Sigma Aldrich (Bornem, Belgium), complete protease inhibitor cocktail from Roche (Vilvoorde, Belgium) and DNAse (Deoxyribonuclease I, Type II from Bovine Pancreas) from Sigma Aldrich (Bornem, Belgium). Phosphate buffered saline (PBS), Dulbecco's Modified Eagle Medium (DMEM), L-glutamine, trypsin and fetal bovine serum were purchased from Lonza (Verviers, Belgium). All other reagents were of analytical grade and obtained from conventional commercial sources.

JPET Fast Forward. Published on October 16, 2019 as DOI: 10.1124/jpet.119.261149
This article has not been copyedited and formatted. The final version may differ from this version.

Human cerebral cortex was obtained from Analytical Biological Services Inc., Wilmington, DE, USA.

Tissue and membrane preparations

Preparation of membrane proteins from rat and human cortex Membrane proteins from rat cortex were prepared as described previously (Fuks 2003). Briefly, after rats were sacrificed by decapitation, brains were removed rapidly and dissected on ice. All subsequent operations were performed at 4°C. Brain tissue, either rat or human cerebral cortex, was homogenized (10% w/v) in 20 mM Tris-HCl buffer (pH 7.4) containing 250 mM sucrose (buffer A). Homogenates were spun at 30,000 g for 15 min and the pellets were resuspended in the same buffer. After incubation at 37°C for 15 min, membranes were washed three times using the same centrifugation protocol. Final pellets were resuspended in buffer A at a protein concentration of 10–15 mg ml^{-1} and stored at -140°C until further use.

Preparation of membrane proteins from HEK and COS-7 cells Human SV2A, B, C were expressed in HEK cells and rat $GABA_AR$ ($\alpha1\beta2\gamma2$; $\alpha2\beta2\gamma2$; $\alpha5\beta2\gamma2$) in COS-7 cells. Cells were subcultured in DMEM containing 200 mM L-glutamine and 100 µg ml^{-1} zeocin, supplemented with 10% fetal bovine serum, and grown in a humidified atmosphere of 5% CO_2 at 37°C. Confluent cells were harvested by trypsinization and pelleted by centrifugation at 1,500 g for 10 min at 4°C. The pellet was washed with ice cold PBS using the same centrifugation protocol, and homogenized in a buffer containing 15 mM Tris-HCl, 1 mM EGTA, 0.3 mM EDTA and 2 mM $MgCl_2$ (pH 7.5) supplemented with complete protease inhibitor cocktail. The homogenate was freeze-thawed twice and equilibrated at 25°C followed by a 10-min DNAse (10 U ml^{-1}) treatment. The solution was centrifuged for 25 min at 40,000 g and 4°C. Finally, the pellet was resuspended in buffer A at a protein concentration of 5–10 mg ml^{-1} and stored at -140°C until further use.

Radioligand binding experiments

Experiments were performed as previously described (Fuks 2003). For all assays, membrane proteins (100 µg per assay for cortical membrane proteins; 70–125 µg for SV2A, 2–5 µg for SV2B, 40–60 µg for SV2C and 75–125 µg for rat $GABA_AR$ subtypes) were incubated for 120 min at 4°C or 60–150 min at 37°C in 0.5 or 2 ml of Tris-HCl buffer (50 mM, pH 7.4) containing 2 mM $MgCl_2$. All glass fiber filters (from Brandel Inc.) used in the experiments were pre-soaked in 0.1% polyethyleneimine.

Competition binding experiments Increasing concentrations of unlabeled competing drugs were added in the presence of 0.9 or 9 nM [^{3}H]PSL, 1 or 4 nM [^{3}H]UCB30889 or 2 nM [^{3}H]flunitrazepam. At the end of the incubation period, membrane-bound radioligand was recovered by rapid filtration through GF/B filters. Plates were washed rapidly three times with 0.3 ml of ice-cold Tris buffer; the total washing procedure did not exceed 10 sec.

Kinetic experiments Specific [^{3}H]PSL binding in association experiments was measured at the indicated times after addition of membrane proteins at 37°C. Dissociation was induced by addition of 10 µM of unlabeled PSL to the association reaction mixture. Samples were filtered on GF/C filters and washed with 5 ml of ice-cold Tris buffer. Total filtration time per sample did not exceed 2 sec.

Saturation binding experiments Membrane proteins were incubated with [^{3}H]PSL at concentrations ranging from 0.05 to 22 nM and samples were filtered using GF/B filters. Nonspecific binding (NSB) was defined as residual binding observed in the presence of 10 µM unlabeled PSL for [^{3}H]PSL,1 mM LEV for [^{3}H]UCB30889 or 10 µM diazepam for [^{3}H]flunitrazepam. Radioactivity was determined by liquid scintillation.

The effect of UCB1244283, a positive allosteric modulator of SV2A, on PSL binding to SV2A was also evaluated. Studies were performed at 4^{o}C according to the protocol described by Wood and Gillard (2017).

In vivo receptor occupancy The protocol developed by Li and colleagues (2006) was followed, using NMRI mice instead of rats. Animals received vehicle (TWEEN/saline) or PSL (10 ml/kg body weight), administered intraperitoneally, followed 27 minutes later by tail-vein injections (2 µl/g) of either [^{3}H]UCB30889 (2 µCi) or [^{3}H]Flunitrazepam (1 µCi). Necks of mice were dislocated 3 mins after injection, and whole brains were rapidly removed, weighed and homogenized in 10 volumes ice-cold Tris buffer. The homogenate (300 µL) was filtered over GF/C filters, and washed 3 times with 2 ml ice-cold Tris buffer. Retained radioactivity was counted by liquid scintillation. Studies consisted of 8 treatment groups (6 PSL doses, 1 vehicle, 1 UCB30889/flunitrazepam), with 6 mice per group.

Selectivity studies

Selectivity of PSL for its therapeutic targets was determined using radioligand binding, receptor activation and electrophysiological studies.

Radioligand binding studies were performed at CEREP (le Bois l'Eveque, France) and at UCB (Braine-l'Alleud, Belgium) according to standard protocols. PSL was evaluated at 10 μM against a panel of various molecular targets including ligand-gated and G-protein coupled receptors, ion channels, transporters and enzymes. Receptors included acetylcholine nicotinic (neuronal bungarotoxin-insensitive), acetylcholine muscarinic (M1, M2 and M3), adenosine (A1 and A2A), epinephrine/norepinephrine (α1A, α2A, β1 and β2), androgen, cannabinoid (CB1 and CB2), cholecystokinin (CCK1), dopamine (D1, D2, D3 and D4), endothelin A (ETA), GABA ($GABA_A$ and $GABA_B$), glycine, glucocorticoid, glutamate (AMPA, kainate and NMDA), neurokinin (NK1, NK2 and NK3), serotonin (5-HT1A, 5-HT1B, 5-HT1D, 5-HT2A, 5HT2B, 5-HT2C, 5-HT3, 5-HT4, 5-HT5A, 5-HT6 and 5-HT7), transforming growth factor beta (TGFβ1), opioid (δ, κ and μ), histamine (H1, H3 and H4), sigma 1 and vasopressin (V1a) receptors. Ion channels included L- and N-type voltage-gated Ca^{2+} channels (Ca_V), voltage-gated Na^+ channels (Na_V) and Ca^{2+}-activated, ATP-sensitive and voltage-gated K^+ (K_V) channels. Other targets were transporters, including adenosine, norepinephrine, dopamine, GABA and 5-HT transporters, as well the enzymes phospholipase A2, cyclooxygenase 1 and 2, constitutive nitric oxide synthase, catechol-O-methyl transferase, GABA transaminase, and tyrosine hydroxylase.

Receptor activation studies were conducted at Eurofins Panlabs (St Charles, MO, USA) using standard protocols. The ability of PSL at concentrations of 1, 3, 10 and 30 μM to activate toll-like receptors (TLR 2 and 4) on cultured human peripheral blood mononuclear cells (PBMCs) was evaluated by measuring concentrations of specific cytokines in the culture supernatant following stimulation. Cytokines tested included interleukin (IL)-1β, IL-6, IL-10, IL-12p40 and tumor necrosis factor α.

The effects of 10 μM PSL on selected ion channels was determined at B'SYS (Witterswil, Switzerland) using standard protocols. These included endogenous Na^+ channels expressed in N1E-115 cells; $Ca_V2.1$, $K_V7.2/7.3$ channels, AMPA receptors (GRIA 1) and kainate receptors (GluK2/GluK5) expressed in CHO cells; $Ca_V3.2$ channels and NMDA (NR1/NR2A, NR1/NR2B) receptors expressed in HEK 293 cells.

Functional electrophysiological studies

Electrophysiological recordings from $GABA_A$ channels were performed as described previously (Ghisdal et al., 2014). Briefly, Cl^- currents were recorded from a CHO-K1 cell line expressing the recombinant human $\alpha1\beta2\gamma2$ $GABA_AR$ subtype. Patch clamp recordings were performed on a PatchXpress system (Molecular Devices). During all procedures, the holding potential was set to –60 mV. Whole-cell compensation was automatically set before each experiment. Current traces were recorded by patch clamp amplifier (Multiclamp 700A Computer-Controlled Patch-Clamp Dual Headstage Amplifier, Axon Instruments) at a sampling rate of 2 KHz. Recordings were performed at room temperature (~25°C).

Data analysis

In radioligand binding studies, data was analyzed by computerized nonlinear curve fitting methods (Graphpad Prism 5 software, San Diego, CA), according to equations describing several binding models (Molinoff et al.,1981). IC_{50} values were corrected to K_i by applying the Cheng and Prusoff equation (Cheng and Prusoff, 1973).

In electrophysiological studies, data was analyzed using DataXpress 2 software (version 2.0.4.2; Molecular Devices, Sunnyvale, CA, USA). The potentiation of $GABA_A$-evoked Cl^- currents in the presence of drug was determined and compared with the maximum potentiation in the presence of 1 μM zolpidem.

JPET Fast Forward. Published on October 16, 2019 as DOI: 10.1124/jpet.119.261149
This article has not been copyedited and formatted. The final version may differ from this version.

RESULTS

Affinity for SV2A and the BZD site

To determine the affinity of PSL for SV2A, the radioligand [^{3}H]UCB30889 was used in competition experiments in human and rat cortex. This compound is a LEV analogue with 20-fold higher affinity for SV2A than LEV, which makes it a suitable radioligand for labeling SV2A (Gillard et al., 2003; Gillard et al., 2006). [^{3}H]Flunitrazepam, a BZD with full agonist properties, was used for determining the affinity of PSL for the BZD site. PSL exhibited nanomolar affinity for SV2A labeled with [^{3}H]UCB30889, and micromolar affinity for the BZD site labeled with [^{3}H]flunitrazepam (Table 1). Further studies on human recombinant $GABA_AR$ subtypes – $\alpha1\beta2\gamma2$, $\alpha2\beta2\gamma2$, and $\alpha5\beta2\gamma2$ – yielded pIC_{50} values of 6.1 ± 0.1 (n=4), >5 (n=3), and 6.0 ± 0.1 (n=3), respectively at 4ºC.

In vivo SV2A and BZD site occupancy

The binding profile of PSL to SV2A and the BZD site was also characterized in vivo, where results were similar to those obtained using cortical preparations – SV2A occupancy was observed at low, and BZD site occupancy at higher doses, indicating greater PSL affinity for SV2A than the BZD site. In the dose-range administered intraperitoneally in mice, PSL ED_{50} for SV2A occupancy was 0.4 µmol/kg (0.2 mg/kg; pED_{50} 6.4 mol/kg), while that of BZD site occupancy was markedly higher at 72 µmol/kg (36 mg/kg; pED_{50} 4.14 mol/kg) (Figure 2).

Binding characteristics at SV2 isoforms

Detailed characterization of PSL binding to the three SV2 isoforms was performed using [^{3}H]PSL, the tritium-radiolabeled compound.

Kinetic experiments

Binding kinetics of [^{3}H]PSL were determined on human recombinant SV2 isoforms expressed in HEK cells and in human and rat cortex at 37°C (Figure 3 and Table 2). [^{3}H]PSL association kinetics were monophasic at all protein sources. Dissociation kinetics were also monophasic for the recombinant SV2 isoforms, but more complex in human and rat cortex, although no clear separation of the phases was evident.

JPET Fast Forward. Published on October 16, 2019 as DOI: 10.1124/jpet.119.261149
This article has not been copyedited and formatted. The final version may differ from this version.

Saturation binding experiments

Saturation binding curves of [^{3}H]PSL on human recombinant SV2A/B/C and on human and rat cortex proteins were compatible with the labeling of a homogenous population of binding sites at 37°C (Figure 4). Corresponding affinities and B_{max} values are given in Table 3. The affinity of [^{3}H]PSL was similar for all protein sources and the K_d value obtained for recombinant human SV2A corresponded with the K_i obtained for the unlabeled compound using [^{3}H]UCB30889 (Table 1).

UCB1244283 is a positive allosteric modulator of SV2A that increases binding of BRV and LEV to the protein (Daniels et al., 2013). Use of the modulator (at 30 μM and at 4ºC) had no effect on the B_{max} for [^{3}H]PSL binding to the human SV2A protein in HEK 293 membranes, but reduced the affinity from 2.3 nM±0.2 (n=3) to 3.90 nM±0.5 ($p<0.05$, Student's t-test).

Competition experiments

Competition experiments were performed on all human recombinant SV2 isoforms expressed in HEK cells and on human and rat cortex proteins using several SV2A ligands, as well as diazepam (Figure 5). These experiments were performed with 0.9 nM [^{3}H]PSL. Data were analyzed using sigmoidal dose-response fits with variable slope and the resulting pIC_{50} values were transformed into pK_i values (Table 4). The affinity of the selective SV2A ligands – LEV, UCB30889 and BRV – was very low for both SV2B and SV2C labeled with [^{3}H]PSL, resulting in incomplete competition curves at the concentration range used. This is in line with previous reports, demonstrating the selectivity of LEV and BRV for SV2A (Gillard et al., 2011, Noyer et al., 1995). Competition with PSL led to a complete displacement of [^{3}H]PSL binding on all protein sources. For all human recombinant SV2 isoforms, the hill slopes of the curve fits were not different from unity and the obtained K_i values for PSL were in agreement with the K_d values of the radiolabeled compound.

In human and rat cortex proteins, the competition curves of LEV, BRV and UCB30889 fitted on the data using a sigmoidal dose-response curve with variable slope were shallower than those for PSL. The corresponding hill coefficients ranged from -0.8 to -0.7 and reached significant difference from unity for LEV on both human and rat cortex proteins ($p<0.01$) and for UCB30889 and BRV on rat cortex ($p<0.01$) (Table 4). The pronounced shallow profile of these competition curves allowed analysis of data with a model describing the binding to two independent populations of binding sites. At a radioligand concentration of 0.9 nM, this resulted in a fit with

85% of the binding sites having an affinity similar to that on recombinant human SV2A, and the remaining sites displaying an affinity in the low mM range. The latter proportion of binding sites most likely represents the SV2B component, given the very low presence of SV2C in the cortex.

Effects in selectivity studies

Selectivity of PSL for its therapeutic targets was determined using radioligand binding, receptor activation and electrophysiological studies.

In radioligand studies, PSL at 10 μM, lacked significant effects (>50%) on a wide variety of molecular targets, including ligand-gated and G-protein coupled receptors, ion channels, transporters and enzymes. The only significant effect was at the BZD binding site of the $GABA_AR$ (87% inhibition), confirming the profile described above. Approximately 50% inhibition of binding to the human NK2 receptor was also observed and subsequently confirmed in a concentration-response study with a pIC_{50} of 5.

In receptor activation assays, PSL at concentrations up to 30 μM failed to elicit release of any of the tested cytokines from human PBMCs, indicating lack of activity on TLR 2 and 4. In electrophysiological studies, PSL at 10 μM had no significant effect on any of the classic AED targets such as voltage-gated ion channels or glutamatergic receptors.

Activity at recombinant $GABA_A$ receptors

In the recombinant human $\alpha1\beta2\gamma2$ $GABA_AR$ subtype, application of GABA resulted in activation of Cl^- currents with an EC_{50} of 15 μM (data not shown). To evaluate the effects of drugs on these GABA-evoked Cl^- currents, an agonist concentration corresponding to its EC_{20} (5 μM) was selected.

PSL, in a concentration range of 1 nM to 30 μM, when added alone for 5 min during preincubation, did not significantly change basal Cl^- currents compared with control (DMSO 0.5%, data not shown), but potentiated Cl^- currents evoked by 5 μM GABA. Potentiation of GABA-induced Cl^- currents was dose dependent with an EC_{50} of 137 nM and a maximal effect reaching 167% (Figure 6).

JPET Fast Forward. Published on October 16, 2019 as DOI: 10.1124/jpet.119.261149
This article has not been copyedited and formatted. The final version may differ from this version.

The relative efficacy of PSL in potentiating $GABA_AR$ Cl^- currents was compared with that of zolpidem, a reference drug included in each experiment. Zolpidem is a full agonist at the BZD site and potentiates GABA [EC_{20}] with a maximal efficacy at 1 μM. The relative efficacy of PSL at 10 μM was 44±16% compared with the maximal response to zolpidem defined as 100%.

DISCUSSION

PSL was developed in a rational drug discovery program initiated to develop a molecule with a novel mode of action aimed at the treatment of patients with drug-resistant epilepsy. Results of experiments described here confirm that PSL is a high affinity pan-SV2 ligand, and acts as a low affinity partial agonist at the BZD site of $GABA_ARs$. Profiling studies also confirmed the lack of effect on typical AED targets such as ion channels, and glutamate receptors, as well as a variety of other CNS targets, including ligand-gated and G-protein coupled receptors, transporters and enzymes.

PSL is the first ligand that interacts with all three SV2 isoforms. In saturation and competition studies, [^{3}H]PSL displayed nM affinity for SV2A, SV2B and SV2C. This was in contrast to LEV and BRV, both displaying marked selectivity for SV2A, and interacting with SV2B and SV2C only at concentrations 100-fold higher than that at which they interacted with SV2A. This was also consistent with the lack of binding of a LEV derivative and of [^{3}H]BRV in mouse brain tissue lacking SV2A (Lynch et al., 2004, Gillard et al., 2011). The high affinity of [^{3}H]PSL for all isoforms was also reflected in kinetic data. [^{3}H]PSL dissociation kinetics were monophasic at human recombinant SV2 isoforms, but more complex in human and rat cortex; most likely due to the labeling of a relatively low fraction of SV2B and SV2A at 0.9 nM [^{3}H]PSL. At this concentration, relatively more SV2A binding sites are labeled since [^{3}H]PSL has a four-fold higher affinity for SV2A (K_d 1.5 nM) than for SV2B (K_d 6.3 nM). Labeling of only a small proportion of SV2B in both human and rat cortex is supported by results of competition experiments; SV2C labelling was not anticipated given its restricted expression in the cortex (see below). Results with LEV and BRV demonstrated labeling of approximately 85% of the binding sites with affinities similar to that at human recombinant SV2A. Finally, both SV2A and SV2B labeling in the cortex is supported by the observation that the B_{max} values for [^{3}H]PSL were approximately twice as high as those observed for SV2A-selective ligands (Gillard et al., 2003; Gillard et al., 2011). Results do not allow an accurate prediction of the SV2A/B ratio in the cortex, since differences in the labeling of both isoforms in native versus recombinant

expression systems cannot be excluded. Overall, results are consistent with the interaction of PSL with all three SV2 isoforms and suggest that it may be a useful ligand in further characterization of these proteins.

The roles of SV2B and SV2C in the pathophysiology of epilepsy remain unknown. Few reports have addressed the role of SV2B, since its distribution in the mammalian brain partly overlaps with that of SV2A (Bajjalieh et al., 1993; Bajjalieh et al., 1994). SV2B -/- mice do not show phenotypic abnormalities and electrophysiological studies on cultured neurons from these mice do not reveal any obvious effects on neurotransmission (Chang et al., 2009; Janz et al., 1999a; Venkatesan et al., 2012). In a recent study, SV2C expression was found to be strongest in the basal ganglia, and more restricted in the cortex of rodent, rhesus macaque, and human brain (Dunn et al., 2019), consistent with results from previous rodent studies (Janz et al., 1999b; Dardou et al., 2011). In human brain, SV2C was highly colocalized with the GABA transporter in the striatum, substantia nigra and ventral tegmental area (Dunn et al., 2019). SV2C expression was weak or absent in the hippocampus of autopsy controls, but increased in biopsies from patients with temporal lobe epilepsy due to mesial temporal sclerosis; in contrast, SV2A and SV2B expression levels were decreased (Crevecoeur et al., 2013). Since PSL has high affinity for all three SV2 isoforms, it could be postulated that binding to SV2B/C in addition to SV2A may contribute to broader, more sustained antiseizure effects.

PSL differs from SV2A-selective ligands not only in its affinity for SV2B and SV2C, but also in its interaction with SV2A, as suggested by the slow kinetics of [^{3}H]PSL and the effect of the modulator, UCB1244283. BRV and LEV have extremely fast kinetics – BRV's dissociation $t_{½}$ is 20 s at 37ºC (Gillard et al., 2011), and that of LEV is 30 s at 25ºC (Noyer et al., 1995). [^{3}H]PSL dissociation $t_{½}$ from human SV2A was 30 minutes at 37ºC. This slower off-rate was also seen in rat and human cortex, suggesting a predominance of SV2A in these tissues. The SV2A positive allosteric modulator, UCB1244283, increases both BRV and LEV binding, but by different mechanisms; an increase in binding capacity for LEV and an increase in binding affinity and capacity for BRV (Wood and Gillard 2017). Allosteric modulation is typically associated with an increase in binding affinity; however, as a putative transporter of the major facilitator superfamily, SV2 can adopt different inward and outward facing conformations (Quistgaard et al., 2016), and with selective binding of some ligands to only one conformation, the presence of an allosteric modulator that stabilizes or induces that specific conformation could seemingly increase binding capacity. The modulator did not significantly increase [^{3}H]PSL binding, but

JPET Fast Forward. Published on October 16, 2019 as DOI: 10.1124/jpet.119.261149
This article has not been copyedited and formatted. The final version may differ from this version.

reduced its affinity for SV2A, suggesting that SV2A may exist in multiple conformational states that can be stabilized by the SV2A modulator, and that the three ligands [^{3}H]LEV, [^{3}H]BRV and [^{3}H]PSL, interact differently with it. Although LEV and BRV exert their therapeutic activity via interaction with SV2A (Matagne et al., 2008), their effect on the protein remains unknown. Therefore, it is difficult to predict the functional consequences of the slow off-rate and the novel mechanism of interaction of PSL with SV2A. Given the evidence that antiseizure potency correlates with SV2A binding affinity (Noyer et al., 1995; Kaminski et al., 2008; Kaminski et al., 2009b; Gillard et al., 2011), it is plausible that such a high-affinity and long-lasting interaction could also lead to improved antiseizure efficacy.

Postsynaptically, PSL displayed low-to-moderate (μM) affinity for the BZD site in human and rat brain membranes with no interspecies difference in potency. Results were similar in recombinant $GABA_AR$ subtypes with α1, α2 and α5 subunits co-expressed with β2 and γ2 subunits. These subunits were chosen as they have been suggested to mediate many of the BZDs' pharmacological effects (D'Hulst et al., 2009). In functional studies, PSL lacked any direct effect on recombinant α1β2γ2 $GABA_ARs$, but potentiated the effects of low GABA concentrations [EC_{20}] giving around 20% of the maximum GABA response) with a pEC_{50} of approximately 7.0 (100 nM). This observation is in keeping with the known mechanism of action of many BZDs – positive allosteric modulators of $GABA_ARs$ that do not open the Cl^- channel on binding, but increase the affinity for channel gating by GABA (Sigel et al., 2012). PSL's relative efficacy compared with zolpidem was 44%, indicating that it acts as a partial agonist. PSL was designed specifically to act as a partial agonist in an effort to minimize the potential for induction of tolerance. BZDs have potent antiseizure effects; however, their long-term use is limited by sedation, tolerance, and the risk of dependence (Riss et al., 2008; Rudolph and Knoflach, 2011; Ochoa et al., 2016). In epilepsy, tolerance is associated with a loss of antiseizure efficacy – a progressive increase in seizure frequency and severity and an increased risk of withdrawal seizures, even if AEDs are kept at constant maintenance doses (Riss et al., 2008; Ochoa et al., 2016). Traditional BZDs such as DZP act as full agonists at the BZD site; partial agonists, however, with lower intrinsic efficacy, could potentially be associated with a lower likelihood of tolerance (Rundfeldt and Löscher, 2014). Approaches to reduce the limitations of BZDs have focused on the development of subtype-selective agents or those with low intrinsic efficacy (Rudolph and Knoflach, 2011; Rundfeldt and Löscher, 2014).

JPET Fast Forward. Published on October 16, 2019 as DOI: 10.1124/jpet.119.261149
This article has not been copyedited and formatted. The final version may differ from this version.

In vivo binding data indicate 50% SV2A and BZD site occupancy at 0.2 and at 36 mg/kg, respectively, supporting in vitro results, with 100-fold lower PSL potency at the BZD site compared with SV2A. In the accompanying report, PSL is shown to be active in a variety of nonclinical seizure and epilepsy models in the 0.1 mg/kg to 10 mg/kg dose range (Leclercq et al., 2019). This corroborates observations that moderate-to-high SV2 occupancy is associated with antiseizure activity and that low-level BZD site occupancy potentiates this effect (Kaminski et al., 2009a).

In conclusion, PSL is a first-in-class AED candidate with a pre- and postsynaptic mechanism of action. Studies described here have shown that PSL displays high affinity for the three SV2 isoforms, ranging from 1.5 to 6.3 nM, and low-to-moderate affinity for the $GABA_AR$ BZD site, where it acts as a partial agonist, and that this profile is maintained in vivo. Furthermore, the interaction of PSL with SV2A differs from that of LEV and BRV, in that it displays a markedly slower dissociation rate and its activity is not potentiated by an SV2A modulator. These additional properties may contribute to the highly active profile of PSL in nonclinical seizure and epilepsy models, including those where the SV2A-selective ligands, LEV and BRV, show limited or no activity (Leclercq et al., 2019).

CONFLICTS OF INTEREST

All authors are current or former employees of UCB Pharma.

ACKNOWLEDGEMENTS

The authors would like to thank John Lambert, David Urbain, Murielle Martini and Veronique Declercq, UCB Pharma, Braine L'Alleud, Belgium, for their skillful technical assistance. The authors also acknowledge Barbara Pelgrims, PhD, UCB Pharma, Brussels, Belgium, for overseeing the development of the manuscript and Azita Tofighy for providing writing support, funded by UCB Pharma.

AUTHORSHIP CONTRIBUTIONS

Participated in research design: M Wood, V Daniels, C Wolff, M Gillard
Conducted experiments: V Daniels
Contributed new reagents or analytic tools: L Provins
Performed data analysis: M Wood, V Daniels, C Wolff, M Gillard

Wrote or contributed to the writing of the manuscript: M Wood, C Wolff, M Gillard, RM Kaminski

REFERENCES

Bajjalieh SM, Frantz GD, Weimann JM, McConnell SK, Scheller RH (1994). Differential expression of synaptic vesicle protein 2 (SV2) isoforms. J Neurosci 14:5223–5235.

Bajjalieh SM, Peterson K, Linial M, Scheller RH (1993). Brain contains two forms of synaptic vesicle protein 2. Proc Natl Acad Sci USA 90:2150–2154.

Bartholome O, Van den Ackerveken P, Sánchez Gil J, de la Brassinne Bonardeaux O, Leprince P, Franzen R, Rogister B (2017). Puzzling out synaptic vesicle 2 family members functions. Front Mol Neurosci;10:148. doi: 10.3389/fnmol.2017.00148.

Chang WP, Sudhof TC (2009). SV2 renders primed synaptic vesicles competent for Ca^{2+}-induced exocytosis. J Neurosci 29:883–897.

Cheng Y, Prusoff WH (1973). Relationship between the inhibition constant (K1) and the concentration of inhibitor which causes 50 per cent inhibition (I50) of an enzymatic reaction. Biochem Pharmacol 22:3099–3108.

Crevecoeur J, Kaminski RM, Rogister B, Foerch P, Vandenplas C, Neveux M, Mazzuferi M, Kroonen J, Poulet C, Martin D, Sadzot B, Rikir E, Klitgaard H, Moonen G, Deprez M (2014). Expression pattern of synaptic vesicle protein 2 (SV2) isoforms in patients with temporal lobe epilepsy and hippocampal sclerosis. Neuropathol Appl Neurobiol 40:191–204.

Crowder KM, Gunther JM, Jones TA, Hale BD, Zhang HZ, Peterson MR, Scheller RH, Chavkin C, Bajjalieh SM (1999). Abnormal neurotransmission in mice lacking synaptic vesicle protein 2A (SV2A). Proc Natl Acad Sci USA 96:15268–15273.

Daniels V, Wood M, Leclercq K, Kaminski RM, Gillard M (2013). Modulation of the conformational state of the SV2A protein by an allosteric mechanism as evidenced by ligand binding assays. Br J Pharmacol 169:1091–1101.

Dardou D, Dassesse D, Cuvelier L, Deprez T, De Ryck M, Schiffmann SN (2011). Distribution of SV2C mRNA and protein expression in the mouse brain with a particular emphasis on the basal ganglia system. Brain Res 1367:130–145.

D'Hulst C, Atack JR, Kooy RF (2009). The complexity of the $GABA_A$ receptor shapes unique pharmacological profiles. Drug Discovery Today 14:866–874.

Dunn AR, Hoffman CA, Stout KA, Ozawa M, Dhamsania RK, Miller GW. Immunochemical analysis of the expression of SV2C in mouse, macaque and human brain (2019). Brain Res 1;1702:85–95.

Fuks B, Gillard M, Michel P, Lynch B, Vertongen P, Leprince P, Klitgaard H, Chatelain P (2003). Localization and photoaffinity labelling of the levetiracetam binding site in rat brain and certain cell lines. Eur J Pharmacol 478:11–19.

Ghisdal P, Noel N, Pacio N, Martini M, Foerch P, Hanon E, Wolff C (2014). Determining the relative efficacy of positive allosteric modulators of the $GABA_A$ receptor: design of a screening approach. J Biomol Screening 19:462–467.

Gillard M, Fuks B, Michel P, Vertongen P, Massingham R, Chatelain P (2003). Binding characteristics of [3H]ucb 30889 to levetiracetam binding sites in rat brain. Eur J Pharmacol 478:1–9.

Gillard M, Chatelain P, Fuks B (2006). Binding characteristics of levetiracetam to synaptic vesicle protein 2A (SV2A) in human brain and in CHO cells expressing the human recombinant protein. Eur J Pharmacol 536:102–108.

Gillard M, Fuks B, Leclercq K, Matagne A (2011). Binding characteristics of brivaracetam, a selective, high affinity SV2A ligand in rat, mouse and human brain: relationship to anti-convulsant properties. Eur J Pharmacol 664:36–44.

Gravielle MC (2016). Activation-induced regulation of $GABA_A$ receptors: Is there a link with the molecular basis of benzodiazepine tolerance? Pharmacol Res 109:92–100.

Janz R, Goda Y, Geppert M, Missler M, Sudhof TC (1999a). SV2A and SV2B function as redundant Ca2+ regulators in neurotransmitter release. Neuron 24:1003–1016.

Janz R, Sudhof TC (1999b). SV2C is a synaptic vesicle protein with an unusually restricted localization: anatomy of a synaptic vesicle protein family. Neuroscience 94:1279–1290.

Kaminski RM, Matagne A, Leclercq K, Gillard M, Michel P, Kenda B, Gillard M, Michel P, Kenda B, Talaga P, Klitgaard H (2008). SV2A protein is a broad-spectrum anticonvulsant target: functional correlation between protein binding and seizure protection in models of both partial and generalized epilepsy. Neuropharmacology 54:715–720.

Kaminski RM, Matagne A, Patsalos PN, Klitgaard H (2009a). Benefit of combination therapy in epilepsy: a review of the preclinical evidence with levetiracetam. Epilepsia 50:387–397.

Kaminski RM, Gillard M, Leclercq K, Hanon E, Lorent G, Dassesse D, Matagne A, Klitgaard H (2009b). Proepileptic phenotype of SV2A-deficient mice is associated with reduced anticonvulsant efficacy of levetiracetam. Epilepsia 50:1729–1740.

Kaminski RM, Gillard M, Klitgaard H (2012). Targeting SV2A for Discovery of Antiepileptic Drugs. In: Noebels JL, Avoli M, Rogawski MA, Olsen RW, Delgado-Escueta AV, editors. Jasper's Basic Mechanisms of the Epilepsies, 4th edition. Bethesda (MD).

Klitgaard H, Matagne A, Nicolas J-M, Gillard M, Lamberty Y, De Ryck M, Kaminski RM, Leclercq K, Niespodziany I, Wolff C, Wood M, Hannestad J, Kervyn S, Kenda B. (2016). Brivaracetam: rationale for discovery and preclinical profile of a selective SV2A ligand for epilepsy treatment. Epilepsia 57:538–548.

Leclerq K, Matagne A, Provins L, Klitgaard H, Kaminski RM (2019) Pharmacological profile of the antiepileptic drug candidate padsevonil – characterization in rodent seizure and epilepsy models. J Pharmacol Exp Ther.

Li J, Fish RL, Cook SM, Tattersall FD, Atack JR (2006). Comparison of in vivo and ex vivo [3H]flumazenil binding assays to determine occupancy at the benzodiazepine binding site of rat brain $GABA_A$ receptors. Neuropharmacol 51:168–172.

Löscher W, Gillard M, Sands ZA, Kaminski RM, Klitgaard H (2016). Synaptic Vesicle Glycoprotein 2A Ligands in the Treatment of Epilepsy and Beyond. CNS Drugs 30:1055–1077.

Lynch BA, Lambeng N, Nocka K, Kensel-Hammes P, Bajjalieh SM, Matagne A, Fuks B (2004). The synaptic vesicle protein SV2A is the binding site for the antiepileptic drug levetiracetam. Proc Natl Acad Sci USA 101:9861–9866.

Matagne A, Margineanu DG, Kenda B, Michel P, Klitgaard H (2008). Anti-convulsive and anti-epileptic properties of brivaracetam (ucb 34714), a high-affinity ligand for the synaptic vesicle protein, SV2A. Br J Pharmacol 154:1662–1671.

Meehan AL, Yang X, McAdams BD, Yuan L, Rothman SM (2011). A new mechanism for antiepileptic drug action: vesicular entry may mediate the effects of levetiracetam. J Neurophysiol 106:1227–1239.

Meehan AL, Yang X, Yuan LL, Rothman SM (2012). Levetiracetam has an activity-dependent effect on inhibitory transmission. Epilepsia 53:469–476.

Mendoza-Torreblanca JG, Vanoye-Carlo A, Phillips-Farfán BV, Carmona-Aparicio L, Gómez-Lira G (2013). Synaptic vesicle protein 2A: basic facts and role in synaptic function. Eur J Neurosci 38:3529–39.

Molinoff PB, Wolfe BB, Weiland GA (1981). Quantitative analysis of drug-receptor interactions: II. Determination of the properties of receptor subtypes. Life Sci 29 427–443.

Noyer M, Gillard M, Matagne A, Henichart JP, Wulfert E (1995). The novel antiepileptic drug levetiracetam (ucb L059) appears to act via a specific binding site in CNS membranes. Eur J Pharmacol 286:137–146.

Quistgaard EM, Löw C, Guettou F, Nordlund P (2016). Understanding transport by the major facilitator superfamily (MFS): structures pave the way. Nat Rev Mol Cell Biol 17:123–132.

Ochoa JG, Kilgo WA (2016). The role of benzodiazepines in the treatment of epilepsy. Curr Treat Options Neurol 18:18. doi: 10.1007/s11940-016-0401-x.

Ohno Y, Tokudome K (2017). Therapeutic Role of Synaptic Vesicle Glycoprotein 2A (SV2A) in Modulating Epileptogenesis. CNS Neurol Disord Drug Targets 16:463–71.

Riss J, Cloyd J, Gates J, Collins S (2008). Benzodiazepines in epilepsy: pharmacology and pharmacokinetics. Acta Neurol Scand 118:69–86.

Rudolph U, Knoflach F (2011). Beyond classical benzodiazepines: novel therapeutic potential of GABA receptor subtypes. Nat Rev Drug Disc 10:685–697.

Rundfeldt C, Löscher W (2014). The pharmacology of imepitoin: the first partial benzodiazepine receptor agonist developed for the treatment of epilepsy. CNS Drugs 28:29–43.

Sigel E, Steinmann ME. Structure, function, and modulation of GABA(A) receptors (2012). J Biol Chem 287:40224–40231.

Tokudome K, Okumura T, Terada R, Shimizu S, Kunisawa N, Mashimo T, Serikawa T, Sasa M, Ohno Y (2016). A Missense Mutation of the Gene Encoding Synaptic Vesicle Glycoprotein 2A (SV2A) Confers Seizure Susceptibility by Disrupting Amygdalar Synaptic GABA Release. Front Pharmacol 7:210. doi: 10.3389/fphar.2016.00210.

Tokudome K, Okumura T, Shimizu S, Mashimo T, Takizawa A, Serikawa T, Terada R, Ishihara S, Kunisawa N, Sasa M, Ohno Y (2016). Synaptic vesicle glycoprotein 2A (SV2A) regulates kindling epileptogenesis via GABAergic neurotransmission. Sci Rep 6:27420. doi: 10.1038/srep27420.

Venkatesan K, Alix P, Marquet A, Doupagne M, Niespodziany I, Rogister B, Seutin V. (2012). Altered balance between excitatory and inhibitory inputs onto CA1 pyramidal neurons from SV2A-deficient but not SV2B-deficient mice. J Neurosci Res 90:2317–2327.

Vinkers CH, Olivier B (2012). Mechanisms underlying tolerance after long-term benzodiazepine use: a future for subtype-selective $GABA_A$ receptor modulators? Adv Pharmacol Sci 2012:416864. doi: 10.1155/2012/416864.

Wood MD, Gillard M (2017). Evidence for a differential interaction of brivaracetam and levetiracetam with the synaptic vesicle 2A protein. Epilepsia 58:255–262.

Yang X, Bognar J, He T, Mohammed M, Niespondziany I, Wolff C, Esguerra M, Rothman SM, Dubinsky JM (2015). Brivaracetam augments short-term depression and slow vesicle recycling. Epilepsia 56:1899–1909.

FOOTNOTES

All studies described in this report were funded by UCB Pharma.

* Current address – Laboratory for Neurobiology and Gene Therapy, Department of Neurosciences KU Leuven, 3000 Leuven, Belgium

† Current address – Roche Innovation Center Basel, F. Hoffmann-La Roche Ltd, 4070 Basel, Switzerland

FIGURE LEGENDS

Figure 1

Structure of padsevonil ((4R)-4-(2-chloro-2,2-difluoro-ethyl)-1-[[2-(methoxymethyl)-6-(trifluoromethyl)imidazo[2,1-b][1,3,4]thiadiazol-5-yl]methyl]pyrrolidin-2-one) compared with the prototypical SV2 ligand, levetiracetam (2S-(2-oxo-1-pyrrolidinyl)butanamide).

Figure 2

In vivo occupancy of synaptic vesicle 2A (SV2A) protein and the benzodiazepine binding site by padsevonil in mouse cortex 30 min after intraperitoneal administration.

Figure 3

Binding kinetics of [^{3}H]padsevonil at 37°C on human recombinant SV2A/B/C expressed in HEK cells and in human and rat cortex. Filled circles represent association and open circles represent dissociation binding kinetics. The curves are the best fit of data obtained using equations describing binding to a single site. Data represent specific binding obtained by subtracting non-specific binding (residual binding in the presence of 10 µM of unlabeled padsevonil) from total binding and have been obtained from at least three independent experiments.

Figure 4

Saturation binding curves of [^{3}H]padsevonil (A) on human cortex and (B) on human recombinant SV2C expressed in HEK cells. Membrane preparations were incubated with increasing concentrations of [^{3}H]padsevonil for 150 min at 37°C. Non-specific binding (NSB) represents residual binding in the presence of 10 µM of padsevonil. Specific binding = total binding – NSB. Data are representative of three independent experiments.

Figure 5

Affinity of compounds for sites labeled with [^{3}H]padsevonil in human recombinant SV2A/B/C proteins and on rat and human cortex. A concentration range of the compounds was incubated with 0.9 nM) [^{3}H]padsevonil for 150 min at 37°C. B0 is the binding of [^{3}H]padsevonil in the absence of any competing compound. Data represent the mean ± standard deviation of at least three independent experiments. Data were normalized to the B0 condition and fitted using a non-linear regression model describing competitive binding to one (straight line) or two (dotted line) binding sites.

Figure 6

Padsevonil potentiates GABA-mediated Cl^- currents in CHO cells stably expressing human $\alpha1\beta2\gamma2$ $GABA_A$ receptor subunits (left panel) by acting as a partial agonist at the benzodiazepine site (right; bar represents standard deviation). Zolpidem, a full agonist, displays a maximal response at 1 μM defined as 100%.

JPET Fast Forward. Published on October 16, 2019 as DOI: 10.1124/jpet.119.261149
This article has not been copyedited and formatted. The final version may differ from this version.

TABLES

Table 1

Affinity of padsevonil for sites labeled with [^{3}H]UCB30889 (SV2A) and [^{3}H]flunitrazepam (benzodiazepine site of the $GABA_A$ receptor) in human and rat cortex at 37°C.

Radioligand	Tissue	pIC_{50}
[^{3}H]UCB30889	Rat cortex	8.43 ± 0.38
	Human cortex	8.97 ± 0.15
[^{3}H]flunitrazepam	Rat cortex	5.50 ± 0.17
	Human cortex	5.80 ± 0.17

Results are the mean ± standard deviation of at least three independent experiments. Data from competition curves were analyzed by non-linear regression using a sigmoidal dose-response model with variable slope.

JPET Fast Forward. Published on October 16, 2019 as DOI: 10.1124/jpet.119.261149
This article has not been copyedited and formatted. The final version may differ from this version.

Table 2

Kinetic constants of [^{3}H]padsevonil binding on human recombinant SV2A/B/C and in human and rat cortex at 37°C.

	SV2A	SV2B	SV2C	Rat cortex	Human cortex
Association	n=4	n=3	n=3	n=3	n=3
K_{on} (nM^{-1}.min^{-1})	0.02 ± 0.01	0.02 ± 0.03	0.04 ± 0.03	0.01 ± 0.004	0.06 ± 0.01
$t_{½}$ (min)	13.9 ± 2.1	4.7 ± 0.8	2.6 ± 0.2	12.4 ± 0.8	7.9 ± 0.7
Dissociation	n=6	n=3	n=3	n=3	n=3
k_{off} (min^{-1})	0.02 ± 0.01	0.13 ± 0.02	0.20 ± 0.02	0.04 ± 0.01	0.04 ± 0.01
$t_{½}$ (min)	29.0 ± 5.8	5.4 ± 0.9	3.6 ± 0.4	16.0 ± 0.4	17.3 ± 2.8
K_D *(nM)*	1	7	7	4	1

k_{off} is the dissociation kinetic constant, k_{on} is the association kinetic constant, and $t_{½}$ is the association or dissociation half-time.

Kinetic constants were calculated by non-linear regression analysis of association and dissociation curves of [^{3}H]PSL as depicted in Figure 3, using a model describing the interaction of a ligand with a single site showing the calculated affinity constant (K_D). Data represent mean ± standard deviation.

JPET Fast Forward. Published on October 16, 2019 as DOI: 10.1124/jpet.119.261149
This article has not been copyedited and formatted. The final version may differ from this version.

Table 3

K_d and B_{max} values of [^{3}H]padsevonil on human recombinant SV2A/B/C and on human and rat cortex at 37°C.

	SV2A	SV2B	SV2C	Rat cortex	Human cortex
K_d (nM)	1.53 ± 0.15	6.34 ± 1.67	2.40 ± 0.16	2.73 ± 1.04	2.11 ± 0.84
B_{max} (pmol/mg)	109.9 ± 3.2	52.8 ± 7.8	23.8 ± 4.6	27.3 ± 9.2	9.3 ± 1.6

Data represent mean ± standard deviation (n=3) and were obtained from the analysis of saturation curves as presented in Figure 4 using a non-linear regression model describing binding to a single site.

JPET Fast Forward. Published on October 16, 2019 as DOI: 10.1124/jpet.119.261149
This article has not been copyedited and formatted. The final version may differ from this version.

Table 4

pK_i values and Hill slopes of selective SV2A ligands and diazepam for sites labeled with 0.9 nM [^{3}H]padsevonil on recombinant human SV2A/B/C and on human and rat cortex at 37°C.

	Levetiracetam	Brivaracetam	UCB30889	Padsevonil	Diazepam
pK_i					
SV2A	5.2 ± 0.1	6.6 ± 0.1	6.7 ± 0.2	8.5 ± 0.1	<5
SV2B	3.1 ± 0.04	<4	<4	7.9 ± 0.1	<5
SV2C	3.2 ± 0.1	4.2 ± 0.1	4.8 ± 0.2	8.5 ± 0.2	5.6 ± 0.1
Human cortex	5.3 ± 0.3	6.4 ± 0.2	6.7 ± 0.2	8.7 ± 0.1	5.9 ± 0.4
Rat cortex	5.0 ± 0.1	6.4 ± 0.1	6.6 ± 0.2	8.7 ± 0.1	<5
Hill slope					
Human cortex	-0.71 ± 0.03	-0.68 ± 0.05	-0.74 ± 0.12	-0.99 ± 0.21	ND
Rat cortex	-0.76 ± 0.03	-0.74 ± 0.26	-0.79 ± 0.15	-0.94 ± 0.13	ND

ND=not determined

Data are presented as mean ± standard deviation (n=3–10) and were obtained from non-linear regression analysis of untransformed raw data using a sigmoidal dose-response model with variable slope. Missing values could not be calculated due to incomplete competition curves as a result of compound solubility limits.

JPET Fast Forward. Published on October 16, 2019 as DOI: 10.1124/jpet.119.261149
This article has not been copyedited and formatted. The final version may differ from this version.

FIGURES

Figure 1

Padsevonil

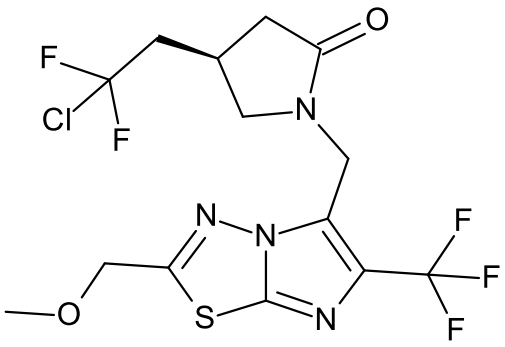

Levetiracetam

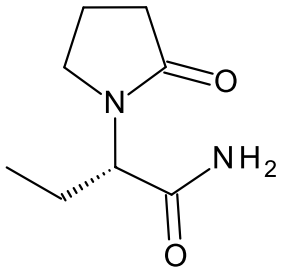

JPET Fast Forward. Published on October 16, 2019 as DOI: 10.1124/jpet.119.261149
This article has not been copyedited and formatted. The final version may differ from this version.

Figure 2

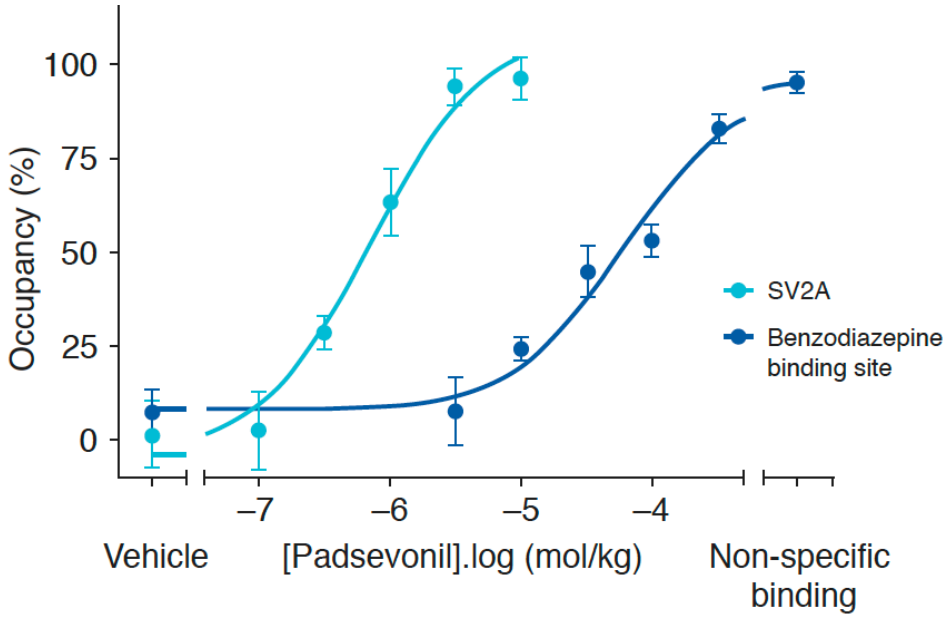

JPET Fast Forward. Published on October 16, 2019 as DOI: 10.1124/jpet.119.261149
This article has not been copyedited and formatted. The final version may differ from this version.

Figure 3

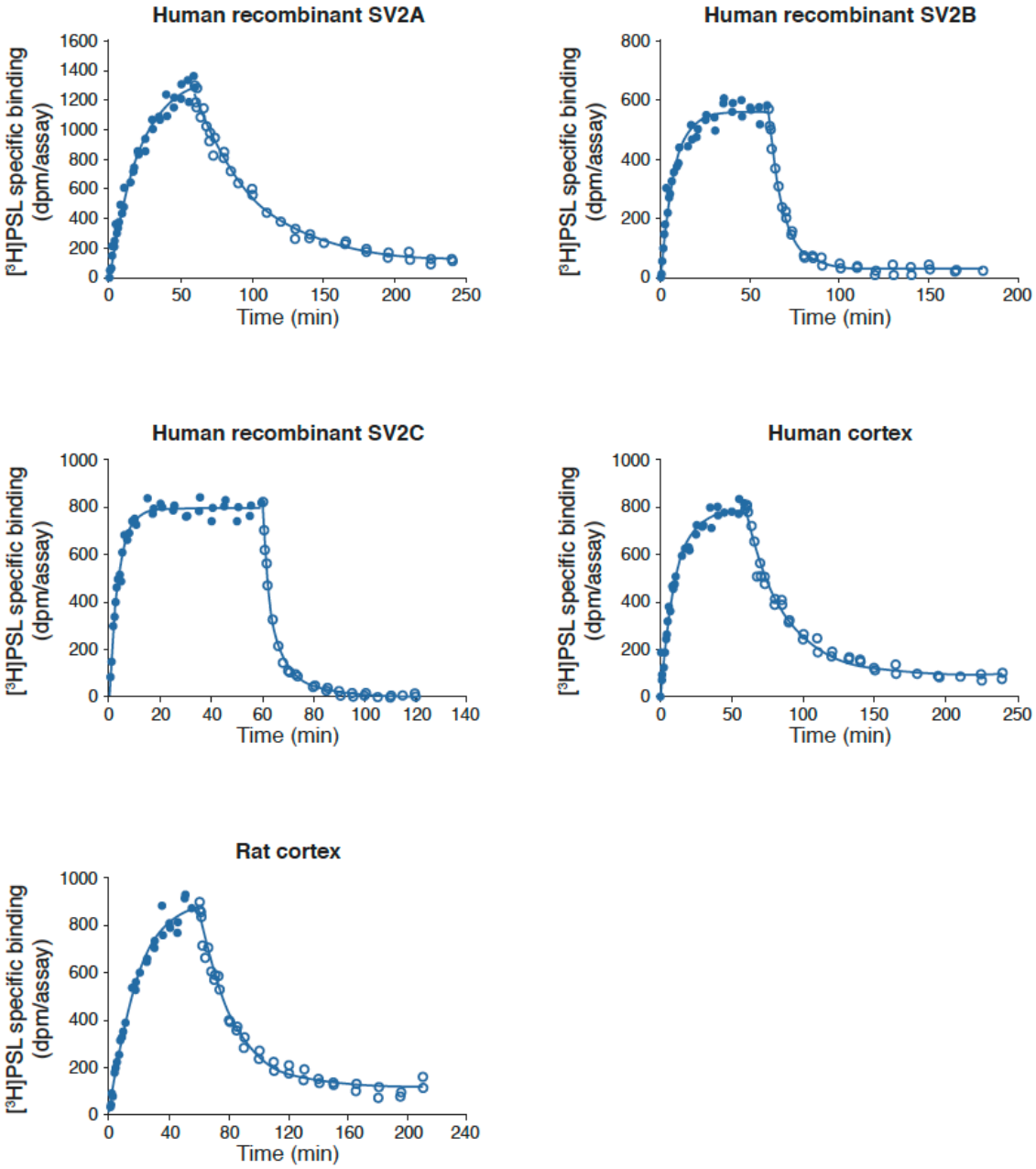

JPET Fast Forward. Published on October 16, 2019 as DOI: 10.1124/jpet.119.261149
This article has not been copyedited and formatted. The final version may differ from this version.

Figure 4

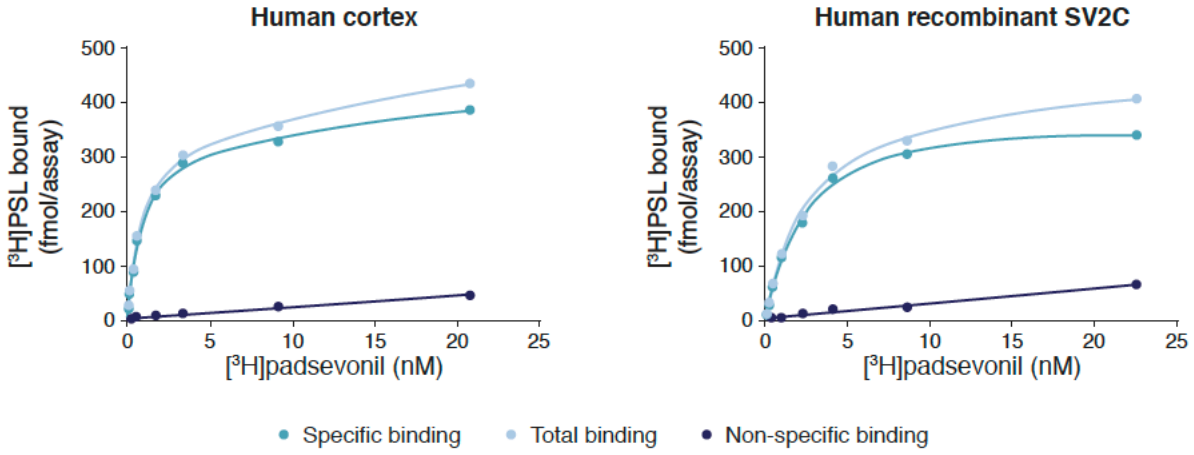

JPET Fast Forward. Published on October 16, 2019 as DOI: 10.1124/jpet.119.261149
This article has not been copyedited and formatted. The final version may differ from this version.

Figure 5

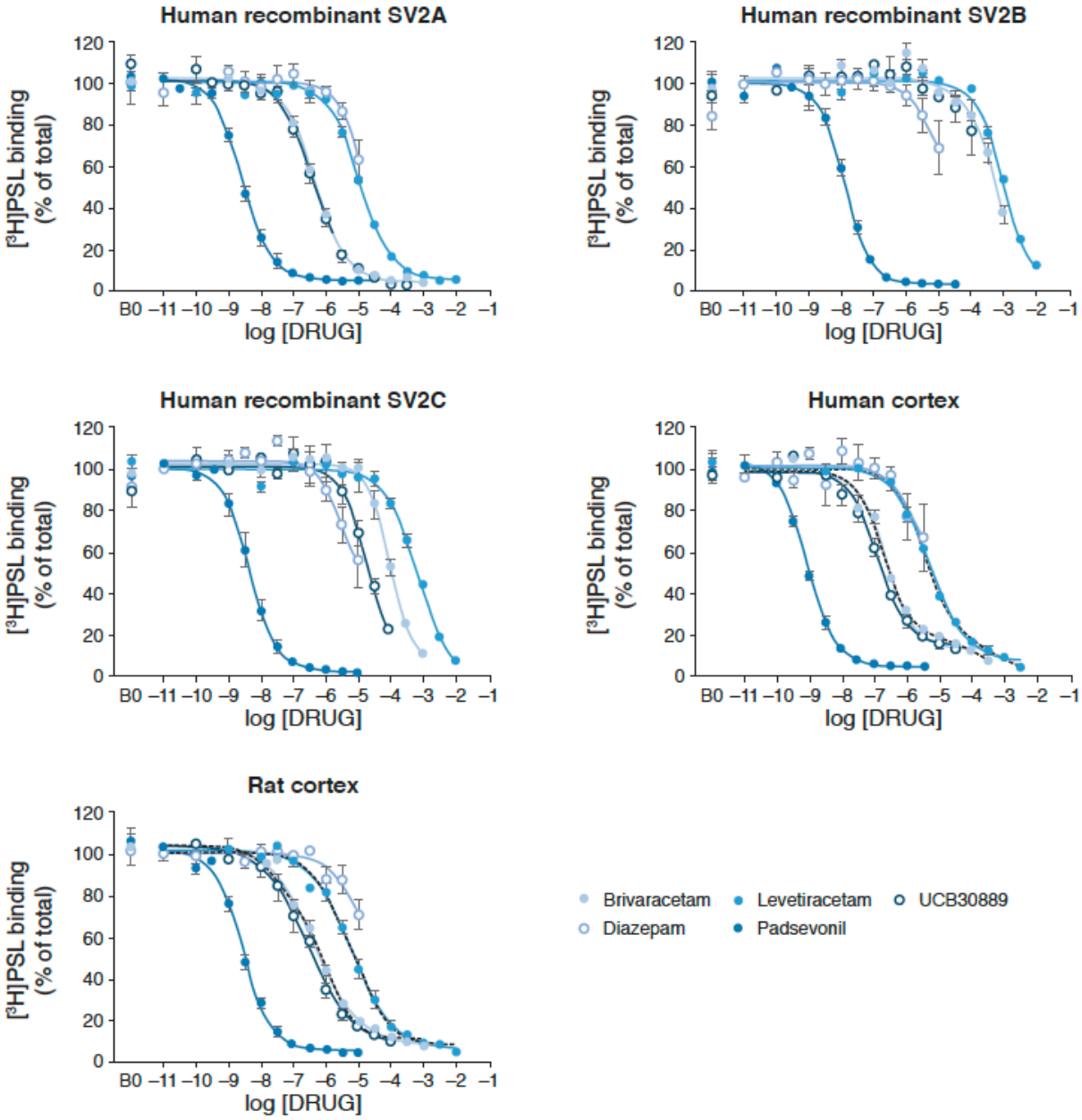

JPET Fast Forward. Published on October 16, 2019 as DOI: 10.1124/jpet.119.261149
This article has not been copyedited and formatted. The final version may differ from this version.

Figure 6